

A Review of the Techniques to Measure the Hermeticity of Glass Frit Encapsulated Solar Cells

Jorge Martins¹, Dzmitry Ivanou², Adélio Mendes^{3*}




¹LEPABE - Laboratory for Process Engineering, Environment, Biotechnology and Energy, Faculty of Engineering, University of Porto, Rua Dr. Roberto Frias, 4200-465 Porto, Portugal (jorgem@fe.up.pt) ORCID [0000-0001-7615-7694](https://orcid.org/0000-0001-7615-7694); ²LEPABE - Laboratory for Process Engineering, Environment, Biotechnology and Energy, Faculty of Engineering, University of Porto, Rua Dr. Roberto Frias, 4200-465 Porto, Portugal (ivanou@fe.up.pt) ORCID [0000-0002-5313-4016](https://orcid.org/0000-0002-5313-4016); ³LEPABE - Laboratory for Process Engineering, Environment, Biotechnology and Energy, Faculty of Engineering, University of Porto, Rua Dr. Roberto Frias, 4200-465 Porto, Portugal (mendes@fe.up.pt) ORCID [0000-0003-2472-3265](https://orcid.org/0000-0003-2472-3265) *corresponding author

Abstract

Emerging 3rd generation photovoltaic technologies such as perovskite and dye-sensitized solar cells are very attractive for commercialization mainly due to their low-cost materials and fabrication processes. The main drawback of these devices is their poor long-term stability. To increase the long-term stability of these devices, a hermetic encapsulation is required. The hermeticity of encapsulated devices are measured and characterized using hermeticity tests according to standard test procedures. A review of the several techniques to measure the hermeticity is presented, addressing the test methods, limitations and applicability to perovskite and dye-sensitized solar cells glass frit encapsulated devices.

Author Keywords. Hermeticity, Leak Rate Detection, Perovskite Solar Cells, Dye-Sensitized Solar Cells.

Type: Research Article

 Open Access  Peer Reviewed  CC BY

1. Introduction

Dye-sensitized solar cells (DSSCs) and perovskite solar cells (PSCs) are included in the emerging third generation of PV technologies. These technologies use low-cost and abundant materials, and can be used for building integrated applications. The mentioned advantages make these PV devices very attractive for commercialization. However, their main disadvantage is the poor long-term stability ([IRENA 2017](#)).

Conventional DSSCs are prepared on conductive glass substrates and consist of a photoanode, a dye, an electrolyte (*i.e.* liquid), and a counter electrode. The leakage of the liquid electrolyte is the main source instability for DSSCs ([Hamann et al. 2008](#)). PSCs are typically fabricated on conductive glass substrates and comprise several layers: an electron transport layer (ETL), a mesoporous scaffold, a perovskite light absorber, a hole transport layer (HTL) and a back contact ([Leijtens et al. 2015](#)). The perovskite light absorber is highly unstable in the presence of moisture and oxygen ([Asghar et al. 2017](#)).

DSSCs and PSSCs must be properly encapsulated to avoid the leakage of electrolyte and to prevent the ingress of moisture and oxygen, thus increasing the long-term stability of the devices. The sealant material must be inert, to avoid the degradation of the components of the cell, and to provide airtight encapsulation through the lifetime of the devices ([Wang et al. 2016](#)).

Widely used sealant materials include thermo-plastics such as surlyn™, ethylene vinyl acetate (EVA) and UV and thermal cure epoxy resins. These materials cannot provide long-term airtight encapsulation (Matteocci et al. 2016).

In recent years, an alternative encapsulation method based on glass frit materials was developed and used to seal DSSCs and PSCs (Emami et al. 2020; Ribeiro et al. 2012; Ivanou et al. 2016; Sastrawan et al. 2006). The glass frit bonding technique uses low melting point glass (< 420 °C) as an intermediate bonding layer to join two substrates. Glass frits are commercialized in form of a paste consisting of fine glass particles, organic binders and solvents (Knechtel, Wiemer, and Frömel 2005).

Glass frit materials have good wettability to most surfaces and can bond rough surfaces (Knechtel 2005). Moreover, these materials are inert, provide an airtight encapsulation and have high bonding strength (Knechtel 2015). These properties make glass frits one of the most ideal sealant material to encapsulate technologies that require hermetic encapsulation, such as the third generation of PV technologies (Emami et al. 2020). Moreover, glass frit bonding can be used for other electronic devices, e.g. microelectromechanical systems (MEMS) (Esashi 2008) and organic light-emitting devices (OLED) (Morena et al. 2018).

The airtightness of an encapsulated package is characterized based on the leakage of the sealant, i.e. the effectiveness of the sealant in preventing exchanges between the sealed cavity and the outside environmental (Kähler, Lofink, and Reinert 2020). The leakage is dependent on the size and the number of leak channels in the sealant perimeter. Leaks are divided into four categories: gross, moderate, fine and ultra-fine based on the measured leak rates. Leak rates above $1 \times 10^{-5} \text{ Pa}\cdot\text{m}^3\cdot\text{s}^{-1}$ are considered gross leaks; moderate leaks have leak rates between $1 \times 10^{-5} \text{ Pa}\cdot\text{m}^3\cdot\text{s}^{-1}$ and $1 \times 10^{-7} \text{ Pa}\cdot\text{m}^3\cdot\text{s}^{-1}$; leak rates from $1 \times 10^{-7} \text{ Pa}\cdot\text{m}^3\cdot\text{s}^{-1}$ to $1 \times 10^{-9} \text{ Pa}\cdot\text{m}^3\cdot\text{s}^{-1}$ are defined as fine leaks; and ultra-fine leaks present leak rates from $1 \times 10^{-9} \text{ Pa}\cdot\text{m}^3\cdot\text{s}^{-1}$ to $1 \times 10^{-11} \text{ Pa}\cdot\text{m}^3\cdot\text{s}^{-1}$. Commonly, leak rates lower than $1 \times 10^{-7} \text{ Pa}\cdot\text{m}^3\cdot\text{s}^{-1}$ are considered hermetic (ASTM 2016; Kähler, Lofink, and Reinert 2020).

There are several procedures to measure the leak rate of packages. Most of these methods are standardized and described in the MIL-STD-883 standard (Department of Defense 2019), MIL-STD-202 standard (Department of Defense 2015), MIL-STD-750 standard (Department of Defense 2012), JESD22-A109-A standard (JEDEC 2001) and ASTM F2391-05 standard (ASTM 2016). A review of the several leak rate measurements methods is presented in this work and their applicability to third generation of PV technologies is discussed.

2. Understanding Leakage Mechanisms

The molecules of a gas move freely with high velocity interacting with each other and with any surface in their path. In a sealed package, the molecules of a gas bump into the package walls, i.e. the substrates and the sealant perimeter. The number of collisions is dependent of the number of molecules of the gas, and is correlated to the pressure and temperature by the ideal gas law (Greenhouse, Lowry, and Romenesko 2012):

$$PV = nRT \quad (1)$$

where, P is pressure, V is volume, n is number of gas molecules, \mathcal{R} is the gas constant and T is the absolute temperature.

Two permeation mechanisms can be identified when a gas is entering or leaving a cavity through a leak channel: viscous flow and Knudsen diffusion. Viscous flow occurs when the gas molecules collide predominantly with each other. Knudsen flow takes place when the gas molecules strike mainly the wall of the leak channel (Sundén and Fu 2017).

The average distance a molecule of a gas travels before colliding with another is called the mean free path (λ). λ is inversely proportional to the pressure of the gas and the diameter of the molecule (Roy et al. 2003). The ratio of λ and the diameter of the leak channel (\varnothing) (considering the leak channel has a shape of a pipe) is known as Knudsen number (K_n) and is used to define the type of flow (Roy et al. 2003):

$$K_n = \frac{\lambda}{\varnothing} \quad (2)$$

For $K_n \leq 0.01$ the viscous flow is the dominant permeation mechanism and the Knudsen diffusion is the principal permeation mechanism for $K_n \geq 10$. For $0.01 < K_n < 10$ both permeation mechanisms contribute for the gas permeation (Roy et al. 2003).

The gas flow rate, q , through a pipe is given by Greenhouse, Lowry, and Romenesko (2012):

$$q = C(P_{out} - P_{in}) \quad (3)$$

where, P_{out} is the total pressure at the outlet of the pipe, P_{in} is the total pressure at the inlet of the pipe and C is the flow conductance. The conductance represents the resistance to the mass transport due to the friction between the molecules and the walls (Greenhouse, Lowry, and Romenesko 2012).

The conductance in the viscous flow regime is proportional to the average pressure. The viscous flow rate in a long round shape tube is given by the Hagen-Poiseuille equation (Greenhouse, Lowry, and Romenesko 2012):

$$q_v = \frac{\pi d^4 P_a}{128 \eta \ell} (P_{out} - P_{in}) \quad (4)$$

where, d is the diameter of the tube, P_a is the average pressure, η is the viscosity of the gas and ℓ is the length of the tube. Viscous flow cannot occur when the pressure inside a cavity is equal to the external pressure. The pressure gradient is the driving force for viscous flow. Thus, packages encapsulated at 1 atm for normal atmospheric use (*i.e.* 1 atm) are not subject to gas permeation by viscous flow (Greenhouse, Lowry, and Romenesko 2012). Viscous flow happens when a pressure difference is imposed to packages and when the leak channels of the sealant are significantly larger than the mean free path of the molecules of a gas. Under these conditions, viscous flow is only presented in gross leaks, *i.e.* leak rates higher than $1 \times 10^{-5} \text{ Pa}\cdot\text{m}^3\cdot\text{s}^{-1}$ (Greenhouse, Lowry, and Romenesko 2012).

In Knudsen diffusion, the conductance is proportional to average velocity of the molecules, thus it is dependent on the molecular mass and the temperature of the gas. The Knudsen diffusion rate in a long round tube is given by Roy et al. (2003):

$$q_m = \frac{\pi d^3}{12 \ell} \sqrt{\frac{8 \mathcal{R} T}{\pi M}} (p_{out} - p_{in}) \quad (5)$$

where, d is the diameter of the tube, ℓ is the length of the tube, M is the molecular mass, \mathcal{R} is universal gas constant, T is temperature and p_{out} and p_{in} are the partial pressure of a specific gas molecule at the outlet and inlet of the pipe. Knudsen diffusion is present when there is a difference in the partial pressure of a gas between the sealed package and the external environment. The Knudsen diffusion mechanism is dominant when the leaking channel is substantially smaller than the mean free path of the molecules of the gas and therefore when leaks rates are lower than $1 \times 10^{-7} \text{ Pa}\cdot\text{cm}^3\cdot\text{s}^{-1}$ (Greenhouse, Lowry, and Romenesko 2012).

The above mentioned equations (Equation (4) and Equation (5)) are used to quantify the leak rate of a sealed package. However, the leak rate changes with the time and pressure (total and partial) and is different for different molecules. In a package encapsulated at 1 atm of N_2 placed in ambient air (1 atm), no viscous flow is present because the total pressure is equal

inside and outside of the package. However, the partial pressure of the N₂ in the package is 1 atm while in the outside is 0.78 atm. Thus, N₂ will leak out until the partial pressure reaches equilibrium. O₂ will leak into the package because the partial pressure of O₂ is 0.21 atm in the air and zero atm inside the package. Over time, the leak rate will decrease due to a decrease in the partial pressure gradient. At equilibrium, the composition of the gas in the package will be the same as in air. The time at which equilibrium is reached will depend on the size of the leak channel of the encapsulation (Greenhouse, Lowry, and Romenesko 2012).

The hermeticity tests consider the leaks physics and can be divided in 2 groups: gross leak tests and fine leak tests. Gross leak tests are intended to test packages for gross leaks where viscous flow is present. Gross leak tests are mostly qualitative tests. Devices with gross leaks cannot be considered hermetic, thus the leak rate values are of no interest. These tests include perfluorocarbon gross leak test, dye penetration test and the weight gain test (Greenhouse, Lowry, and Romenesko 2012).

Fine leak tests evaluate if a package have fine leaks and can be characterized as hermetic. The fine leak testing methods are expensive and require specific equipment. Helium leak rate test and Krypton-85 leak test are some of the techniques to measure fine leaks. Most of the fine leak test methods require an additional gross leak analysis. Devices with gross leaks can pass the fine leak tests, thus showing false positives (Kähler, Lofink, and Reinert 2020).

3. Leak Rate Measurement Methods

3.1. Gross leak tests

3.1.1. Perfluorocarbon gross leak test

The perfluorocarbon gross leak test consists in immersing the device in type I detector fluid and pressurizing the chamber for a defined time. The type I detector fluid is a perfluorocarbon liquid with a boiling temperature between 50 °C and 95 °C. The bombing (pressurization) conditions are presented in Table 1 (Department of Defense 2019).

Pressure / Pa	Minimum pressurization time / hour	
	Test condition C1	Test condition C3
2.07 × 10 ⁵	23.5	12
3.10 × 10 ⁵	8	4
4.14 × 10 ⁵	4	2
5.17 × 10 ⁵	2	1
6.21 × 10 ⁵	1	0.5
7.24 × 10 ⁵	0.5	N/A

Table 1: Pressurization conditions for perfluorocarbon gross leak test
 (adapted from Department of Defense (2019))

In test condition C1, after the bombing phase, the device is removed from the chamber with the type I detector fluid and placed on a second chamber with a type II indicator fluid at 125 ± 5 °C. The type II indicator fluid is a perfluorocarbon liquid with a boiling temperature from 140 °C to 200 °C. The device must be observed from the moment of the immersion for a minimum period of 30 second, unless rejected earlier. If a stream of bubbles or two or more large bubbles originate from the same point the device is rejected (Department of Defense 2019).

Due to the difficulty in detecting the bubbles, the observation step must use a magnifier and a nonreflective black background while the device is illuminated (Department of Defense 2019).

In test condition C3, after the bombing phase, the device is placed in a chamber at $125 \pm 5 \text{ }^\circ\text{C}$ connected to a perfluorocarbon vapor detector that measure the amount of the type I detector fluid that evaporates. Devices where the equipment detects more than $0.167 \text{ }\mu\text{L}$ of type I detector fluid have gross leaks ([Department of Defense 2019](#)).

The perfluorocarbon gross leak test involves temperatures that are not compatible with the DSSCs and PSCs. Some of the components of these solar cells are temperature sensitive and degrade at temperatures higher than $85 \text{ }^\circ\text{C}$ ([Mesquita, Andrade, and Mendes 2019](#)).

3.1.2. The weight gain test

The weight gain test identifies if a package has a gross leak by measuring the weight difference of the package before and after being immersed in a fluid under pressure. The weight of the device is measured after a pre-heating step at $125 \text{ }^\circ\text{C}$ for a minimum of 1 hour. The device is then placed in a chamber and immersed in a detector fluid, *e.g.* a perfluorocarbon fluid with boiling point between $50 \text{ }^\circ\text{C}$ and $110 \text{ }^\circ\text{C}$. The chamber is pressurized to $5.17 \times 10^5 \text{ Pa}$ for 2 hours. Devices that cannot withstand this condition can be submitted to $3.10 \times 10^5 \text{ Pa}$ for 10 hours. After the bombing phase, the weight of the devices is measured within 4 minutes following the removal from the fluid. The weight gain of the device is then calculated ([Department of Defense 2019](#)).

Devices with an internal volume of $\leq 0.01 \text{ cm}^3$ and $> 0.01 \text{ cm}^3$ are rejected if they gain more than 1 mg and 2 mg, respectively ([Department of Defense 2019](#)). This test method includes a heating step, similar to the perfluorocarbon gross leak test, that is not compatible with the PSCs and DSSCs.

3.1.3. Penetrant dye test

The penetrant dye test is a destructive test that is used to determine the location of gross leaks. The devices are place in a chamber filled with dye and the chamber is pressurized to *ca.* $7.24 \times 10^5 \text{ Pa}$ for a minimum of 3 hours. The bombing condition of $4.14 \times 10^5 \text{ Pa}$ for 10 hours can also be used. After bombing step, the devices are washed using a suitable solvent for the particular dye used in the test. Afterwards, the devices are examined under an ultraviolet light source using a magnifier for any evidence of dye penetration. The detection of dye inside a package is considered a failure ([Department of Defense 2019](#)).

The MIL-STD-883 define that the dyes Zyglo, Fluorescein and Rhodamine B with maximum reflection at 365 nm, 493.5 nm and 556 nm, respectively, shall be used ([Department of Defense 2019](#)).

This test cannot be used to determine the gross leaks of encapsulated PV devices since it is a destructive test. Any device, hermetic or non-hermetic, will become non-functional.

3.2. Fine leak tests

3.2.1. Helium leak rate test

The helium leak rate test is the most used test to characterize the hermeticity of several types of electronic devices. This test uses helium as a tracer gas to measure the fine leaks of packages. Helium is a suitable tracer gas because is one of the smallest molecules, is inert, non-toxic and has a low concentration in air. This test method is comprised of two phases, a bombing phase and a measurement phase. In the bombing phase, the devices are placed in a chamber and pressurized to a specific pressure of helium for a certain time. Only helium must be present in the chamber, therefore, the chamber must be evacuated before filling with helium. Otherwise, a series of vents and helium refills can be performed. During this step,

helium will enter the package cavity due to partial pressure difference (Department of Defense 2019).

After the bombing phase, the chamber is depressurized, and the devices are transferred to a second chamber connected to a mass spectrophotometer. The second chamber is evacuated, forcing the helium that entered the cavity of the package in the bombing phase to leak out. The amount of helium that leaks out is measured by the mass spectrophotometer (Department of Defense 2019).

This technique has two test method: a fixed method and a flexible method. The fixed test method defines the bombing pressure and period (t_1), the maximum dwell time to measure the sample after bombing phase (t_2), the internal volume of the device (V) and the reject leak rate limit (R_1) in $\text{Pa}\cdot\text{m}^3\cdot\text{s}^{-1}$. These conditions are presented in Method 1014 of MIL-STD-883 standard. Devices with leak rates lower than the reject leak rate limit are considered hermetic (Department of Defense 2019).

In the flexible test method, it is possible to choose the bombing period (t_1), the dwell time for the measurement of helium leak rate (t_2) after depressurization and the bombing pressure (P_E), provided that it is $\geq 2.03 \times 10^5$ Pa of helium. The reject helium leak rate limit (R_1), in $\text{Pa}\cdot\text{m}^3\cdot\text{s}^{-1}$ He, is calculated by the Howl-Mann Equation (6) with the previous chosen values, the internal cavity volume of the device and the equivalent leak rate limit (L) (Table 2). The devices are considered hermetic if the measured helium leak rate (R) by the mass spectrometer is lower than the calculated reject helium leak rate limit (R_1) (Department of Defense 2019).

$$R_1 = \frac{LP_E}{P_0} \left(\frac{M_A}{M_{He}} \right)^{\frac{1}{2}} \left\{ 1 - e^{-\left[\frac{Lt_1(M_{Air})}{VP_0(M_{He})} \right]^{\frac{1}{2}}} \right\} e^{-\left[\frac{Lt_2(M_{Air})}{VP_0(M_{He})} \right]^{\frac{1}{2}}} \quad (6)$$

where R_1 is the reject helium leak rate limit in $\text{Pa}\cdot\text{m}^3\cdot\text{s}^{-1}$ He, L is the equivalent leak rate limit in $\text{Pa}\cdot\text{m}^3\cdot\text{s}^{-1}$ air, P_E is the bombing pressure in Pa, P_0 is the atmospheric pressure in Pa, M_{Air} is the molecular weight of air in grams, M_{He} is the molecular weight of tracer gas He in grams, t_1 is the bombing period in seconds, t_2 is the dwell time for the measurement of helium leak rate after depressurization in seconds and V is the internal cavity volume.

Internal cavity volume (V) / cm^3	L reject limit / $\text{Pa}\cdot\text{m}^3\cdot\text{s}^{-1}$ air (for Hybrid Class H, and Monolithic Classes B, S, Q and V*)	L reject limit / $\text{Pa}\cdot\text{m}^3\cdot\text{s}^{-1}$ air (for Hybrid Class K*)
≤ 0.05	5×10^{-9}	1×10^{-10}
$0.05 < V \leq 0.4$	1×10^{-8}	5×10^{-10}
> 0.4	1×10^{-7}	1×10^{-9}

* Equivalent leak rate limits (L) for the various classes of microcircuits

Table 2: Equivalent leak rate limits (L) for all fine leak methods
 (adapted from Department of Defense (2019))

The helium leak rate test has several limitations. This method does not differentiate between helium leaking from a package and desorption of helium from the test chamber surface. The mass spectrophotometer reads the total amount of helium removed from the test chamber. This problem is especially important for packages composed by polymers substrates or sealants, due to high adsorption of helium in these materials. In these cases, it is possible that the leak rate measurement is reading only the desorption of helium, thus providing an inaccurate value (Costello, Desmulliez, and McCracken 2012).

The helium leak rate test is not adequate for very small volume packages. Several authors already discussed the applicability of the helium leak rate test for testing low volume cavities and concluded that false positive results can occur (Tao and Malshe 2005; Goswami and Han 2008; Costello, Desmulliez, and McCracken 2012). The applicability of this test is further conditioned by the strength of the devices to endure the pressure difference that are submitted during bombing and measuring phase. Devices under pressure or vacuum are subject to a force that is related to the bombing/vacuum pressure and the area of the device. Large areas devices ($\geq 7 \times 7 \text{ cm}^2$) can suffer mechanical failure due to the high applied forces, making it impossible to read the leak rate (Emami et al. 2019).

Moreover, high bombing pressures during bombing phase can generate 'one-way' leaks, *i.e.* leak channels induced by the bombing pressure that do not exist under normal conditions. The 'one-way' leaks can provide false hermeticity results (Costello, Desmulliez, and McCracken 2012).

Lastly, the helium leak rate test only measures fine leaks. A device with a gross leak can pass the helium leak rate test, therefore a complementary leak test must be performed to test for gross leaks (Department of Defense 2019).

3.2.2. Cumulative helium leak test (CHLT)

The cumulative helium leak test is a variation of the helium leak rate test. The test procedure is the same as in the helium leak rate test. The main difference is the use of an additional cryogenic pump in the detection system. A cryogenic pump is capable of extracting all of the gases in the test chamber except noble gases which include helium (Greenhouse, Lowry, and Romenesko 2012). If a device has a gross leak, the volume of helium in the test chamber increases rapidly at the start of the test. If a device has a fine leak, the volume of helium increases slowly over time. The rate of change in the volume of helium is used to determine the leak rate. This determination method allows to measure gross and fine leaks. This test is capable of measuring leak rates from $1 \text{ Pa}\cdot\text{m}^3\cdot\text{s}^{-1}$ to $4 \times 10^{-15} \text{ Pa}\cdot\text{m}^3\cdot\text{s}^{-1}$ (Department of Defense 2019). The CHLT has a higher sensitivity compare to the traditional helium leak rate test ($1 \times 10^{-13} \text{ Pa}\cdot\text{m}^3\cdot\text{s}^{-1}$) (Kähler, Lofink, and Reinert 2020). Moreover, virtual leaks due to helium desorption of the surface of a package can be detected through signal reading. Real leaks have a linear rate while virtual leaks exhibit an exponential rate. However, CHLT, like the helium leak rate test, is dependent on the volume of the packages (Kähler, Lofink, and Reinert 2020). The fixed bombing conditions (pressure and time) for different internal volume cavities and the related reject leak rate limits can be found on method 1014.17 of MIL-STD-883 standard. The flexible method can also be used; this method is similar to the flexible method in the helium leak rate test (Department of Defense 2019).

3.2.3. Krypton-85 radioactive tracer gas test

The radioisotope element krypton-85 is used as a tracer gas in the Krypton-85 radioactive tracer gas test. Krypton-85 is a radioisotope with a half-life of *ca.* 11 years and when decays it emits beta and gamma rays (Costello, Desmulliez, and McCracken 2012; Greenhouse, Lowry, and Romenesko 2012). The gamma rays can penetrate package walls, thus the krypton-85 that leaks inside the package can be read by measuring the gamma radiation. The measuring step does not require vacuum to force the tracer gas to leak out as in the helium leak rate test. Kr-85 radioactive tracer gas test is independent of cavity volume and is more suitable industry application where is necessary to test high number devices. The main disadvantage of this method is the use of radioactive material that requires specialized handling. Moreover, over

time the testing apparatus becomes radioactive. This test must be complemented with a gross leak test (Costello, Desmulliez, and McCracken 2012).

Activity of the radioisotope is measured in microcuries per atmosphere cubic centimeter. The concentration of Kr-85 in the tracer gas mixture of Kr-85/air needs to be higher than 1000 $\mu\text{Ci}\cdot\text{Pa}^{-1}\cdot\text{m}^{-3}$. Curie, Ci, is a unit of radioactivity of a material. The devices are placed in a chamber and the chamber is filled with the tracer gas mixture up to a certain pressure for a period determined by Department of Defense (2019):

$$Q_s = \frac{r}{sk(P_e^2 - P_i^2) 3600t} \quad (7)$$

where Q_s is the maximum allowed leak rate in $\text{atm}\cdot\text{cm}^3\cdot\text{s}^{-1}$ Kr-85 (based on L values from Table 2. $1.71 \text{ Pa}\cdot\text{m}^3\cdot\text{s}^{-1}$ Kr-85 = $1 \text{ Pa}\cdot\text{m}^3\cdot\text{s}^{-1}$ air), r is the counts per minute above the ambient background after pressurization, s is the specific activity in $\mu\text{Ci}\cdot\text{Pa}^{-1}\cdot\text{m}^{-3}$ of the Kr-85 tracer gas, k is the counting efficiency of the scintillation crystal used to measure Kr-85 (This k-factor must be determined for the combination of scintillation crystal used for the measurement with the device geometry), P_e is the bombing pressure in Pa (must be higher than 2.03×10^5 Pa), P_i is the original internal pressure of the device in Pa and t is the pressurization period in hours.

After the bombing step, the devices are removed from the chamber and, within 1 hour, the counts per minute must be measured using a scintillation crystal system. The actual Kr-85 leak rate (Q) of a tested device is given by Department of Defense (2019):

$$Q = \frac{\text{Actual read of counts per minutes} \times Q_s}{r} \quad (8)$$

A device is considered hermetic if Q is lower than Q_s .

3.2.4. Optical leak test

The optical leak test is based on the measurement of the deflection of a package when submitted to pressure difference. To use this test the package must be able to deflect at least $7.25 \times 10^{-7} \mu\text{m}\cdot\text{Pa}^{-1}$ (Department of Defense 2019). The package is placed in a chamber where a pressure difference (by vacuum or pressurization) is applied and an interferometer measures the deflection of the package over time. When a device with a leak is pressurized, it will bend inwards. Then, as the gas leak into the package and the pressure starts to equalize, the curve begins to decrease. If a device with a leak is placed under vacuum, first will bend outwards because the pressure is higher inside the package. Then starts to bend inwards as the gas leaks out. By measuring the deflection over time, it is possible to determine the leak rate. The leak rate of the device is given by Equation (9). The deflection stiffness ($\mu\text{m}\cdot\text{Pa}^{-1}$) of a non-leaking sample must be measured to obtain accurate leak rates (Department of Defense 2019).

$$O_L = \frac{V}{TP_a} \times -\ln\left(\frac{\Delta P_f}{\Delta P_i}\right) \quad (9)$$

where, O_L is the implied leak rate of the test in $\text{Pa}\cdot\text{m}^3\cdot\text{s}^{-1}$, V is the internal free volume of the package cavity in m^3 , t is the test duration time in seconds, P_a is the chamber test pressure in Pa as a function of altitude, ΔP_i is the chamber test pressure in Pa at the of the test, ΔP_f is the chamber test pressure – leakage in Pa (Leakage is the change in pressure inside the package during the test. Leakage = deflection movement (μm) / deflection stiffness ($\mu\text{m}\cdot\text{Pa}^{-1}$)).

This test can measure gross and fine leaks. A package fails the gross leak test if no deflection is detected or if the package deflects in the beginning of the test but quickly returns to the unpressurized position. A package passes the fine leak test if the O_L is lower than the values presented in Table 2 (Department of Defense 2019).

The lid of the package must be able to deflect otherwise the optical leak test cannot be applied. Furthermore, this technique has sensitivity issues since it depends on the stiffness and thickness of the lid, the geometry of the sealed cavity, the test duration and the sensitivity of the measuring equipment (optical interferometer). The optical leak test has lower sensibility than other hermeticity methods being able to read leak rates $> 1 \times 10^{-10} \text{ Pa}\cdot\text{m}^3\cdot\text{s}^{-1}$ (Costello, Desmulliez, and McCracken 2012).

3.2.5. Fourier transform infrared spectroscopy (FTIR)

This method uses Fourier transform infrared spectroscopy (FTIR) to determine the concentration of a gas inside a device. The concentration is measured through the absorption of infrared radiation (IR) by the molecules of the gas. A reference FTIR measurement is performed to identify the IR spectrum of the cavity of a package before the test. The test begins by pressurizing the devices using a tracer gas, similar to helium leak rate test. The bombing conditions are arbitrary and should be chosen so that enough tracer gas enters the device. Typically, N_2O is used as tracer gas due to similar molecule size to N_2 and high absorbance in the IR spectrum. Others tracer gases such as SF_6 , OCS , HCl , H_2S can be used instead of N_2O , however most of the mentioned gases are toxic (Veyrié et al. 2005).

After bombing, FTIR is used to measure the concentration of N_2O in the package and monitored its variation over time. The package walls must be transparent to the IR radiation to use this method (Veyrié et al. 2005).

To determine the leak rate, the transmission spectrum of the device after bombing is divided by the transmission spectrum of the reference (before bombing). Thus, transmission rate of the tracer gas in the package is obtained. The partial pressure (p) of the tracer gas is calculated from the transmission rate by Lellouchi et al. (2010):

$$-\log(T') = \frac{\omega l}{RT} p \quad (10)$$

where, T' is the transmission rate for the absorption wavelength of the tracer gas, l is the cavity thickness, ω is the molar coefficient of the gas for the specified wavelength, R is the universal gas constant and T is the temperature.

Lastly, the leak rate (L) is determined using the modified Howl-Mann Equation (11). The rejected leak rate limits for this test are shown in Table 2 (Lellouchi et al. 2010).

$$p = P_E \left\{ 1 - e^{-\left[\frac{Lt_1}{VP_0} \left(\frac{M_{Air}}{M} \right)^{\frac{1}{2}} \right]} \right\} e^{-\left[\frac{Lt_2}{VP_0} \left(\frac{M_{Air}}{M} \right)^{\frac{1}{2}} \right]} \quad (11)$$

where p is the partial pressure of the tracer gas, L is the equivalent leak rate limit in $\text{Pa}\cdot\text{m}^3\cdot\text{s}^{-1}$ air, P_E is the bombing pressure in Pa, P_0 is the atmospheric pressure in Pa, M_{Air} is the molecular weight of air in grams, M is the molecular weight of tracer gas in grams, t_1 is the bombing period in seconds, t_2 is the dwell time for the measurement after depressurization in seconds and V is the internal cavity volume.

The FTIR method can measure leak rates up to $1 \times 10^{-13} \text{ Pa}\cdot\text{m}^3\cdot\text{s}^{-1}$. FTIR measurements can suffer from noise and interference peaks due to reflection of the IR signal in the cavity of the package. Moreover, this test is not standardized and a gross leak test must be performed to rule out gross leaks (Costello, Desmulliez, and McCracken 2012).

The applicability of FTIR technique to determine the hermeticity of glass frit encapsulated solar cells is limited. Solar cells are frequently fabricated on glass substrates. Glass is a material with high transmittance in the visible and near-infrared spectrum up to 3 000 nm and low transmittance from 3 000 nm up to 4 600 nm (Rubin 1985). Most tracer gases used in the FTIR

method have absorption peaks in the infrared region between 2 500 nm and 20 000 nm (Lellouchi et al. 2010). The small wavelength region overlapped limits the tracer gases that can be used and make the test more susceptible to noise and interference.

3.2.6. Residual gas analysis (RGA)

The residual gas analysis is used to measure and quantify the gas elements present inside sealed devices. This test allows to measure the encapsulation atmosphere, the moisture and oxygen content inside the device and the presence of bombing gases of previous tests. Other gases, such as CO₂, CH₄ and NH₃, and other solvents can be identified. A mass spectrophotometer is used to analyzed all the gases (Department of Defense 2019).

Prior to the test, the devices must be preconditioned at 100 °C for 16 - 24 h. The device must be transferred to the testing apparatus within 5 minutes after the prebaking step (Department of Defense 2019).

The testing apparatus is composed of vacuum chamber with an opening connected directly to the mass spectrophotometer. The chamber must be heated to the preconditioned temperature of 100 °C. Moreover, the chamber must contain a piercing mechanism that can pierce the testing sample. This test method is destructive (Department of Defense 2019).

The sample is placed on the vacuum chamber at 100 °C and the chamber is evacuated to a vacuum level which ensures no background interference. The package is then pierced, allowing the gas in the cavity to escape and flow into the mass spectrophotometer for analysis. A device is considered a failure if the pressure difference in the chamber during testing is greater than ± 15 %, which can indicate a non-hermetic device or the piercing was not accomplished (Department of Defense 2019).

The RGA test is expensive, time demanding and requires expert analysis of the results. Moreover, the volume of the devices is limited by the testing apparatus (Costello, Desmulliez, and McCracken 2012).

RGA is not appropriate for characterizing the hermeticity of packages due to its destructive nature. However, it can be used to analyze the long-term stability of the encapsulated devices. As long as the encapsulation is hermetic, the degradation byproducts of solar cells are trapped inside of the sealed cavity and can be identify by RGA. Therefore, this test method is appropriate for solar cells research laboratories (Kähler, Lofink, and Reinert 2020).

4. Conclusion

Hermeticity tests are used to measure and characterize the hermeticity of glass frit encapsulated perovskite solar cells and dye-sensitized solar cells devices. Devices with leak rates lower than $1 \times 10^{-7} \text{ Pa}\cdot\text{m}^3\cdot\text{s}^{-1}$ are considered hermetic. The hermeticity test are divided in gross and fine leak tests. The gross leak tests include the perfluorocarbon gross leak test, the weight gain test and penetrant dye test. These tests cannot be use to qualify the gross leakage of encapsulated solar cells due to high temperatures requirements and its destructive nature of the tests. The fine leak tests include the helium leak rate test, cumulative helium leak test (CHLT), Krypton-85 radioactive tracer gas test, optical leak test, Fourier transform infrared spectroscopy (FTIR) test and residual gas analysis (RGA).

RGA is a destructive test; therefore, it is not suitable to measure the hermeticity of devices. A common limitation of the other tests is the use of a bombing phase that can produce 'one-way' leaks that normally do not exist in normal conditions. Moreover, none of the tests considers the mechanical stress applied to the devices under the bombing phase or vacuum

measurement phase in the case of the helium leak rate test and CHLT. The mechanical stress limits the application of the tests to relatively small area devices ($< 7 \times 7 \text{ cm}^2$).

The more suitable test method is the Fourier transform infrared spectroscopy (FTIR) test. This test has good sensitivity and can use non-toxic tracer gases. However, the test is not standardized, requires complementary gross leak test and is limited by the transmittance of the glass substrates where the solar cells are fabricated.

Future work should focus in the development of a standard test procedure for the FTIR test method and development of a hermeticity test for large area devices suitable for application in the industry.

References

- Asghar, M. I., J. Zhang, H. Wang, and P. D. Lund. 2017. "Device stability of perovskite solar cells – A review". *Renewable and Sustainable Energy Reviews* 77: 131-46. <https://doi.org/10.1016/j.rser.2017.04.003>.
- ASTM. 2016. *Standard test method for measuring package and seal integrity using helium as the tracer gas*. ASTM F2391-05. West Conshohocken, PA.
- Costello, S., M. P. Y. Desmulliez, and S. McCracken. 2012. "Review of test methods used for the measurement of hermeticity in packages containing small cavities". *IEEE Transactions on Components, Packaging and Manufacturing Technology* 2, no. 3 (march): 430-38. <https://doi.org/10.1109/tcpmt.2011.2176122>.
- Department of Defense. 2012. *Test method standard - Environmental test methods for semiconductor devices – Part 1: Test methods 1000 through 1999*. MIL-STD-750-1. Military and Government Specs & Standards (Naval Publications and Form Center) (NPFC).
- . 2015. *Test method standard for electronic and electrical component parts*. MIL-STD-202, Revision H. Military and Government Specs & Standards (Naval Publications and Form Center) (NPFC).
- . 2019. *Test method standard for microcircuits*. MIL-STD-883, Revision L. Military and Government Specs & Standards (Naval Publications and Form Center) (NPFC).
- Emami, S., J. Martins, D. Ivanou, and A. Mendes. 2020. "Advanced hermetic encapsulation of perovskite solar cells: the route to commercialization". *Journal of Materials Chemistry A* 8, no. 5: 2654-62. <https://doi.org/10.1039/c9ta11907h>.
- Esashi, M. 2008. "Wafer level packaging of MEMS". *Journal of Micromechanics and Microengineering* 18, no. 7 (august). <https://doi.org/10.1088/0960-1317/18/7/073001>.
- Greenhouse, H., R. Lowry, and B. Romenesko. 2012. *Hermeticity of electronic packages*. William Andrew. <https://doi.org/10.1016/C2009-0-64380-4>.
- Goswami, A., and B. Han. 2008. "On the applicability of MIL-Spec-based helium fine leak test to packages with sub-micro liter cavity volumes". *Microelectronics Reliability* 48, no. 11-12 (november): 1815-21. <https://doi.org/10.1016/j.microrel.2008.07.067>.
- Hamann, T. W., R. A. Jensen, A. B. F. Martinson, H. Van Ryswyk, and J. T. Hupp. 2008. "Advancing beyond current generation dye-sensitized solar cells". *Energy & Environmental Science* 1, no. 1: 66-78. <https://doi.org/10.1039/b809672d>.
- IRENA - International Renewable Energy Agency. 2017. "REthinking Energy 2017: Accelerating the global energy transformation". <https://www.irena.org/publications/2017/Jan/REthinking-Energy-2017-Accelerating-the-global-energy-transformation>.

- Ivanou, D. K., R. Santos, J. Maçaira, L. Andrade, and A. Mendes. 2016. "Laser assisted glass frit sealing for production large area DSCs panels". *Solar Energy* 135 (october): 674-81. <https://doi.org/10.1016/j.solener.2016.06.043>.
- JEDEC. 2001. *Hermeticity*. JESD22-A109-A. JEDEC Solid State Technology Association.
- Kähler, D., F. Lofink, and W. Reinert. 2020. "Hermeticity tests". In *Handbook of silicon based MEMS materials and technologies*, edited by M. Tilli, M. Paulasto-Krockel, M. Petzold, H. Theuss, T. Motooka and V. Lindroos, 833-43. Elsevier. <https://doi.org/10.1016/B978-0-12-817786-0.00042-6>.
- Knechtel, R. 2005. "Glass frit bonding: An universal technology for wafer level encapsulation and packaging". *Microsystem Technologies* 12, no. 1-2: 63-68. <https://doi.org/10.1007/s00542-005-0022-x>.
- . 2015. "Glass frit bonding". In *Handbook of silicon based MEMS materials and technologies*, edited by M. Tilli, T. Motooka, V.-M. Airaksinen, S. Franssila, M. Paulasto-Kröckel and V. Lindroos, 611-25. 2nd ed.: William Andrew Publishing. <https://doi.org/10.1016/B978-0-323-29965-7.00031-2>.
- Knechtel, R., M. Wiemer, and J. Frömel. 2005. "Wafer level encapsulation of microsystems using glass frit bonding". *Microsystem Technologies* 12, no. 5 (april): 468-72. <https://doi.org/10.1007/s00542-005-0036-4>.
- Leijtens, T., G. E. Eperon, N. K. Noel, S. N. Habisreutinger, A. Petrozza, and H. J. Snaith. 2015. "Stability of metal halide perovskite solar cells". *Advanced Energy Materials* 5, no. 20 (october): Article number 1500963. <https://doi.org/10.1002/aenm.201500963>.
- Lellouchi, D., J. Dhennin, X. Lafontan, D. Veyrie, J.-F. Le Neal, and F. Presseccq. 2010. "A new method for the hermeticity testing of wafer-level packaging". *Journal of Micromechanics and Microengineering* 20, no. 2: Article number 025031. <https://doi.org/10.1088/0960-1317/20/2/025031>.
- Matteocci, F., L. Cinà, E. Lamanna, S. Cacovich, G. Divitini, P. A. Midgley, C. Ducati, and A. Di Carlo. 2016. "Encapsulation for long-term stability enhancement of perovskite solar cells". *Nano Energy* 30 (december): 162-72. <https://doi.org/10.1016/j.nanoen.2016.09.041>.
- Mesquita, I., L. Andrade, and A. Mendes. 2019. "Temperature impact on perovskite solar cells under operation". *ChemSusChem* 12, no. 10 (may): 2186-94. <https://doi.org/10.1002/cssc.201802899>.
- Morena, R. M., J. F. Bayne, J. T. Westbrook, S. Widjaja, and L. Zhang. 2018. "Frit sealing of OLED displays". In *Handbook of organic light-emitting diodes*, edited by C. Adachi, R. Hattori, H. Kaji and T. Tsujimura, 1-22. Springer Japan. https://doi.org/10.1007/978-4-431-55761-6_24-1.
- Ribeiro, F., J. Maçaira, R. Cruz, J. Gabriel, L. Andrade, and A. Mendes. 2012. "Laser assisted glass frit sealing of dye-sensitized solar cells". *Solar Energy Materials and Solar Cells* 96, no. 1 (january): 43-49. <https://doi.org/10.1016/j.solmat.2011.09.009>.
- Roy, S., R. Raju, H. F. Chuang, B. A. Cruden, and M. Meyyappan. 2003. "Modeling gas flow through microchannels and nanopores". *Journal of Applied Physics* 93, no. 8 (april): 4870-79. <https://doi.org/10.1063/1.1559936>.
- Rubin, M. 1985. "Optical properties of soda lime silica glasses". *Solar Energy Materials* 12, no. 4 (september-october): 275-88. [https://doi.org/10.1016/0165-1633\(85\)90052-8](https://doi.org/10.1016/0165-1633(85)90052-8).
- Sastrawan, R., J. Beier, U. Belledin, S. Hemming, A. Hinsch, R. Kern, C. Vetter, et al. 2006. "A glass frit-sealed dye solar cell module with integrated series connections". *Solar Energy*

Materials and Solar Cells 90, no. 11 (july): 1680-91.
<https://doi.org/10.1016/j.solmat.2005.09.003>.

Sundén, B., and J. Fu. 2017. "Low-density heat transfer: Rarefied gas heat transfer". In *Heat transfer in aerospace applications*, 45-70. Academic Press. <https://doi.org/10.1016/B978-0-12-809760-1.00004-1>.

Tao, Y., and A. P. Malshe. 2005. "Theoretical investigation on hermeticity testing of MEMS packages based on MIL-STD-883E". *Microelectronics Reliability* 45, no. 3-4 (march): 559-66. <https://doi.org/10.1016/j.microrel.2004.08.004>.

Veyrié, D., D. Lellouchi, J. L. Roux, F. Pressecq, A. Tetelin, and C. Pellet. 2005. "FTIR spectroscopy for the hermeticity assessment of micro-cavities". *Microelectronics Reliability* 45, no. 9-11 (september): 1764-69. <https://doi.org/10.1016/j.microrel.2005.07.091>.

Wang, D., M. Wright, N. K. Elumalai, and A. Uddin. 2016. "Stability of perovskite solar cells". *Solar Energy Materials and Solar Cells* 147 (april): 255-75. <https://doi.org/10.1016/j.solmat.2015.12.025>.

Acknowledgments

Jorge Martins is grateful to the Portuguese Foundation for Science and Technology (FCT) for their Ph.D. grants (references: SFRH/BD/147201/2019). Jorge Martins is grateful to Seyedali Emami for the contributions in the preparation of this work. The authors acknowledge the Projects: i) POCI01-0145-FEDER-006939, funded by the European Regional Development Fund (ERDF), through COMPETE2020 – Programa POCI and by national funds through FCT and ii) POCI-01-0247-FEDER-017796, “WinPSC” co-funded by ERDF, through COMPETE 2020, under the PORTUGAL 2020 Partnership Agreement. This work was financially supported by: Base Funding - UIDB/00511/2020 of the Laboratory for Process Engineering, Environment, Biotechnology and Energy – LEPABE - funded by national funds through the FCT/MCTES (PIDDAC). Part of this work was also performed under the project SunStorage “Harvesting and storage of solar energy”, with reference POCI01-0145-FEDER-016387.